07

Terahertz generation in a-Si:H/c-Si geterostructures under excitation by femtosecond laser pulses

© A.V. Andrianov[1], E.I. Terukov[1–3], S.N. Abolmasov[1,3]

[1] Ioffe Institute, St. Petersburg, Russia
[2] ITMO University, St. Petersburg, Russia
[3] R&D Center of Thin Film Technologies in Energetics under the Ioffe Institute LLC, St. Petersburg, Russia
E-mail: alex.andrianov@mail.ioffe.ru

Received October 17, 2025
Revised December 18, 2025
Accepted December 22, 2025

The results of studying the generation of terahertz (THz) radiation in a-Si:H/c-Si-based $p-n$-heterostructures photoexcited by femtosecond laser radiation with wavelengths of 400 and 800 nm are presented. A several-times increase in the differential efficiency of THz generation was observed in switching from long-wave to short-wave pumping. Broadening of the THz radiation amplitude spectrum and increase in its upper limit frequency (at the level of 0.01 from the maximum) to about 2.7 THz were also observed.

Keywords: terahertz radiation, heterostructures, femtosecond laser excitation, second harmonic, fast photocurrent.

DOI: 10.61011/TPL.2026.04.63210.20535

In the last few decades, terahertz (THz) time-domain spectroscopy (THz-TDS) has been rapidly developing and finding new areas of application. The method is based on generation and detection of THz-radiation by using femtosecond laser pulses and fast Fourier transform of the THz-radiation waveforms [1–5]. Studies of mechanisms for the THz-radiation generation in semiconductors and development of new types of THz emitters based on them are an important part of THz research [6,7].

Studies [8,9] revealed and examined THz-generation in the a-Si:H/c-Si-based $p-n$-heterostructures due to excitation of a fast photocurrent of nonequilibrium charge carriers created in the region of the structure potential barrier by the 800 nm femtosecond laser radiation. Fast photocurrent emits THz-electromagnetic waves. The structures studied in [8,9] were at the same time quite efficient solar cells. It was found out that intensity of the THz-radiation generated in reverse-biased a-Si:H/c-Si $p-n$-heterostructures is comparable to THz-radiation from InAs crystals which are widely used as emitters in THz-TDS systems (see, e. g., [10–12]). This fact indicates that a-Si:H/c-Si-based solar cells may also be of interest for application in THz-technologies. For instance, large-area THz-emitters may be built based on them. Along with this, radiation of the 800 nm femtosecond pump laser, which was used in [8,9] for THz generation, is not optimal: such pumping does not provide excitation of non-equilibrium carriers in the layer of amorphous silicon. In addition, the exciting-light absorption length in the crystalline silicon layer is about 12 μm [13], which is significantly larger than the size of the electric field localization region in the studied structures even at the reverse bias voltages of several tens of volts.

This paper presents the results of studying THz generation in the a-Si:H/c-Si $p-n$-heterostructures under excitation by second-harmonic radiation of the femtosecond titanium-sapphire laser (photoexcitation wavelength of 400 nm). The study revealed a several-times increase in the THz-generation differential efficiency in switching from the first to second harmonic of the pump laser radiation.

The experiments were performed on the a-Si:H/c-Si $p-n$-heterostructures fabricated according to the procedure described in detail in [14] and on those similar to ones investigated in [9]. Fig. 1 presents the layout of the experiment setup. Radiation of the femtosecond titanium-sapphire laser (pulse duration of about 15 fs, repetition rate of 80 MHz, central wavelength of 800 nm, maximum average power of about 220 mW) was converted into the second harmonic by using a BBO (barium borate oxide) crystal plate 0.15 mm thick (AO LLS). Then, after passing a filter based on SZS-21 glass which cuts off the laser radiation first harmonic, the 400 nm radiation was focused on the surface of the structure under study from the side of the $(p)a$-Si:H/$(n)c$-Si heterojunction in the gap between the metal (Ag) contact grid strips (Fig. 2, a). Fig. 2, a presents the structure under study with compositions and sizes of its layers. Fig. 2, b schematically shows the distributions of total electric field and intensity of the exciting laser radiation in the structure. The size of photoexcitation region was about 200 μm, p-polarized excitation laser radiation was incident on the structure at an angle close to 45°. THz-radiation from the a-Si:H/c-Si $p-n$-heterostructures was collected in the direction of specular reflection from the structure surface and detected by electro-optical gating of the THz-radiation waveforms [2] in the (110) ZnTe wafer using the lock-in technique. The studies were conducted at room temperature in the open air with humidity of about 56 %.

Fig. 3, a shows the characteristic waveform of THz radiation generated in the studied structures under pumping

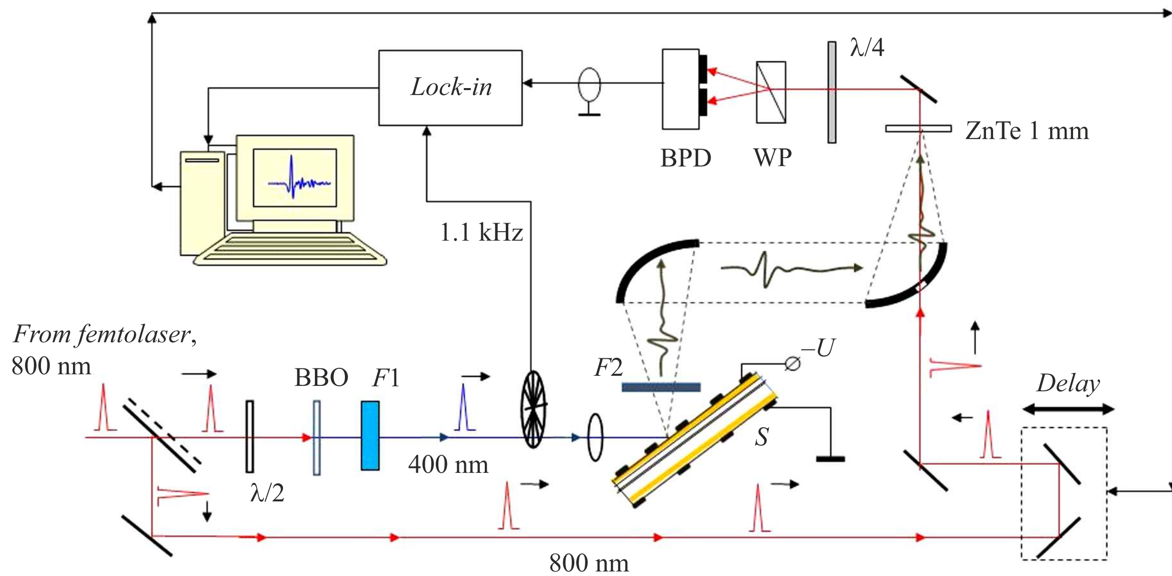

Figure 1. Schematic diagram of the experimental setup. BBO — a plate of nonlinear optical crystal β-BaB_2O_4; $\lambda/2$ and $\lambda/4$ — half-wave and quarter-wave plates, respectively, for the wavelength of 800 nm; $F1$ — filter based on glass SZS-21; $F2$ — black-polyethylene filter, WP — Wollaston prism; BPD — balanced photodiode detector; *Delay* — computer-controlled optical delay line; S — structure under study, to which the bias voltage is applied.

by 400 nm femtosecond laser pulses, reverse bias voltage of 9 V, and average exciting radiation power of 11 mW (the maximum second-harmonic power of the titanium-sapphire laser that could be obtained with the available BBO crystal). Here is also presented the THz-signal characteristic waveform for the structures excited by radiation with the wavelength of 800 nm at the same reverse bias and average photoexcitation power of about 70 mW at which, as per [9], the effect of the electric field dynamic screening in the structures is still insignificant, and THz radiation signal remains virtually linear in the exciting radiation power. Fig. 3, *b* presents amplitude spectra of the THz radiation. The spectra manifest the effect of THz radiation absorption in water vapor, as well as the effect of reflections of THz radiation generated in the structure from its internal layers.

Fig. 4, *a* demonstrates the dependence of the THz-signal amplitude (the amplitude of positive spike in the THz radiation waveform) on the average power of the 400 nm exciting radiation at the reverse bias voltage of 9 V. Evidently, this dependence is almost linear in the range of photoexcitation intensities used in this experiment.

Data presented in Fig. 3, *a* allows us to conclude that, in the case of pumping the structure under study with the 400 nm radiation, THz generation efficiency g_{THz} which may be defined as $g_{\text{THz}} = S_{\text{THz}}/P_{exc}$ (S_{THz} is the detected THz radiation signal, P_{exc} is the exciting radiation power) is significantly higher than in the case of photoexcitation with the 800 nm radiation. The increase in the THz-generation efficiency is about 2.4.

As shown in Fig. 3, *b*, amplitude spectrum of the THz radiation generated in the structures is wider when the photoexcitation wavelength is 400 nm than when it is 800 nm (the spectrum half-width (FWHM) increases from about 0.7 THz to about 1.1 THz). Besides this, the THz generation spectrum at short-wave pumping extends to frequencies of about 2.7 THz (this upper limit frequency corresponds to the level of 0.01 from the maximum).

Indeed, the THz radiation signal will increase with increasing 400 nm pumping power to above 11 mW but, probably, will also reach saturation or even decrease due to the effect of electric field dynamic screening [9]. Determining the optimal power of the 400 nm exciting radiation, i. e. the pump power at which the THz generation signal is maximum, is a separate task that is beyond the scope of this study.

An increase in the THz generation efficiency in the a-Si:H/c-Si-based $p-n$-heterostructures due to transition from the femtosecond pump wavelength of 800 nm to that of 400 nm is caused by two factors. First, in the case of short-wave pumping, generation of nonequilibrium carriers also occurs in the amorphous silicon layer, which leads to an increase in the fast photocurrent responsible for THz radiation. Second, in the case of the 400 nm photoexcitation the pump penetration depth into the c-Si layer is about 0.2 μm [15]. Thus, almost all nonequilibrium carriers created in this layer participate in creating fast photocurrent since they all arise in the region of electric field localization even at bias voltages close to zero.

Fig. 4, *b* shows a characteristic dependence of the THz signal amplitude on the bias voltage on the studied $p-n$-heterostructure under excitation by the 400 nm radiation. As shown, the THz generation signal increases with increasing reverse bias; however, this increase is more gradual than in the case of pumping wavelength

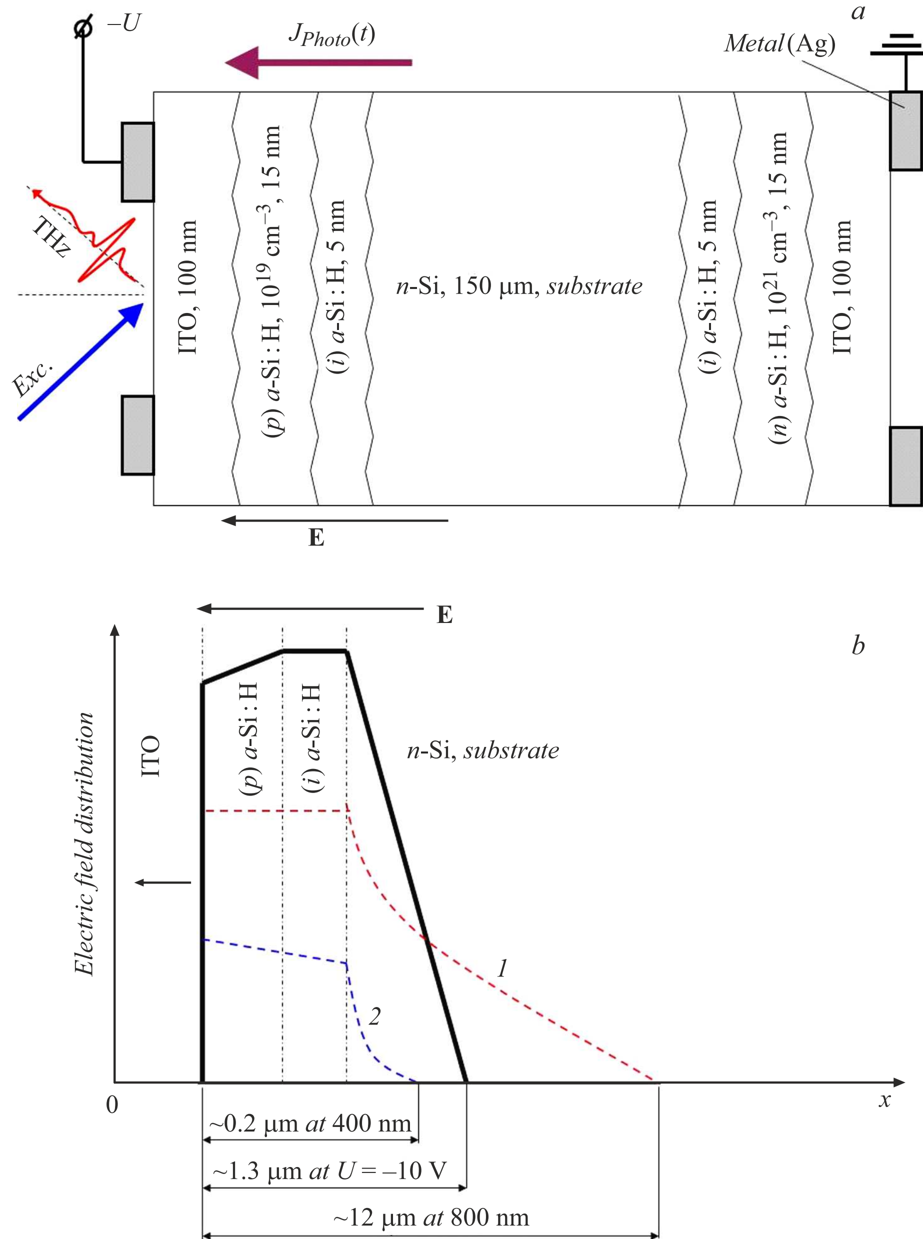

Figure 2. *a* — schematic diagram of the studied *a*-Si:H/*c*-Si *p*—*n*-heterostructure under reverse bias, as well as compositions and thicknesses of its layers. The structure has been formed on a double-sided textured *n*-silicon substrate with resistivity of 1.5 Ω · cm. *b* — schematic distributions of the structures' total electric field **E** (solid bold line) and intensity of the exciting laser radiation (dashed lines) with wavelengths of 800 (*1*) and 400 nm (*2*). Penetration depths of the exciting laser radiation with wavelengths of 800 and 400 nm into the structure were taken from literature [13,15] (the *a*-Si:H bandgap is about 1.8 eV [14]); the size of the total electric field localization region was obtained from estimates.

of 800 nm [9]. In this case, a noticeable THz radiation signal is observed at zero bias. A weak THz signal is also observed at a small forward bias (about 1 V). The observed dependence of the THz radiation signal on bias voltage is also caused by that, in almost the entire range of bias voltages, nonequilibrium carriers are generated in a region whose size is smaller than that of the region of electric field localization in the structure. Therefore, the observed increase in the THz signal amplitude with increasing bias voltage is mainly associated with an increase in the nonequilibrium carriers' acceleration and speed of motion with increasing electric field in the structure.

Thus, the paper presents the results of studying the terahertz radiation generation in the *a*-Si:H/*c*-Si-based *p*—*n*-heterostructures under photoexcitation by femtosecond laser pulses with the wavelengths of 400 and 800 nm. It has been established that, when the structures are excited by radiation with the 400 nm wavelength, the THz-generation differential efficiency increases several times compared to that in the case of the 800 nm photoexcitation. The

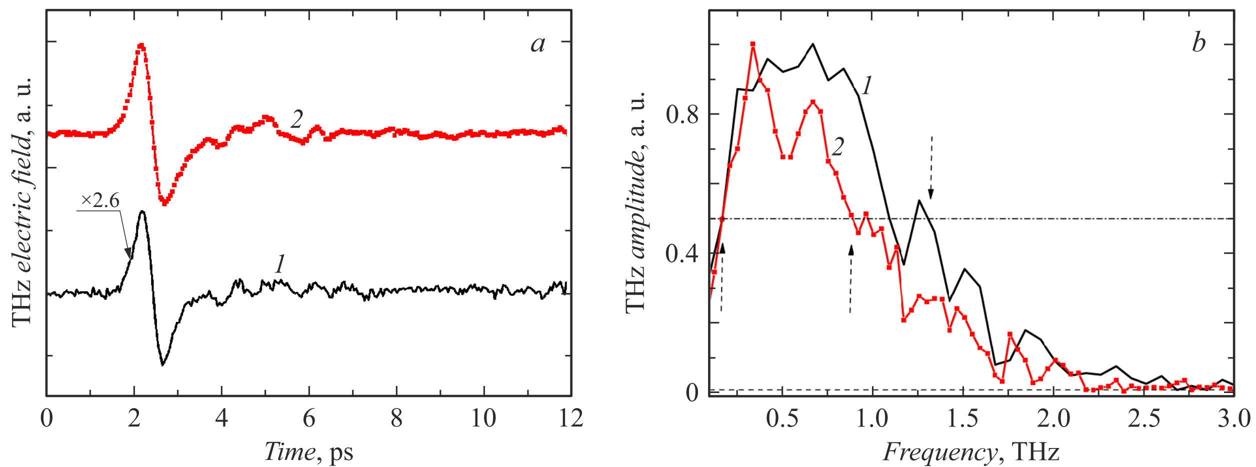

Figure 3. *a* — characteristic waveforms of THz radiation generated in the *a*-Si:H/*c*-Si *p*–*n*-heterostructure at the reverse bias voltage of 9 V under femtosecond laser excitation. Curve *2* is shifted vertically for clarity. *b* — THz radiation amplitude spectra normalized to the maximum. Spectral resolution is 0.1 THz. The dashed line corresponds to the signal level of 0.01 from the maximum, the dash-dotted line corresponds to that of 0.5 from the maximum. Arrows indicate the frequencies at which the THz signal reaches the level of 0.5 from the maximum. *1* — excitation wavelength of 400 nm, average excitation power of 11 mW. *2* — excitation wavelength of 800 nm, average excitation power of 70 mW..

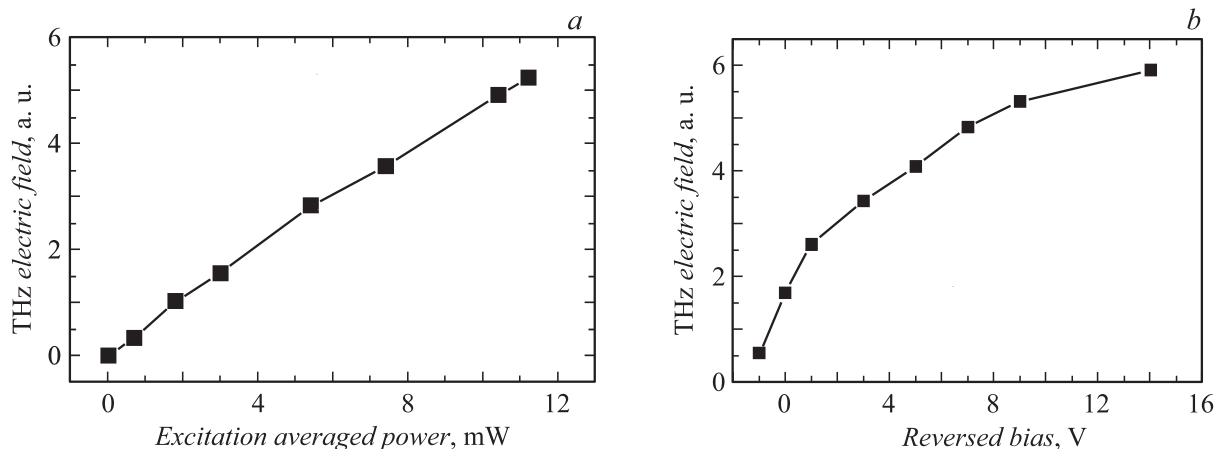

Figure 4. *a* — THz signal amplitude dependence on the average power of the 400 nm exciting radiation at the reverse bias of 9 V. *b* — THz signal amplitude dependence on the bias voltage on the structure. Photoexcitation wavelength is 400 nm, average power is 11 mW.

increase in the THz-generation efficiency under short-wave photoexcitation of structures is associated with more efficient excitation of nonequilibrium electrons and holes in the structure regions where the electric field is concentrated, which ultimately leads to enhancement of fast photocurrent responsible for generating the THz-radiation. In addition, broadening of the THz radiation amplitude spectrum and increase in its upper limit frequency (at the level of 0.01 from the maximum) to about 2.7 THz were observed.

Acknowledgements

The authors express their gratitude to A.O. Zakharyin for useful discussion of the article.

Funding

The study was partially supported by the Russian Science Foundation, project 24-62-00022.

Conflict of interests

The authors declare that they have no conflict of interests.

References

[1] *Terahertz spectroscopy and imaging*, ed. by K.-E. Peiponen, J.A. Zeitler, M. Kuwata-Gonokami (Springer, Berlin–Heidelberg, 2013). DOI: 10.1007/978-3-642-29564-5

[2] J. Neu, C.A. Schmuttenmaer, J. Appl. Phys., **124**, 231101 (2018). DOI: 10.1063/1.5047659

[3] J.F. Lampin, G. Mouret, S. Dhillon, J. Mangeney, Photoniques, **101**, 33 (2020). DOI: 10.1051/photon/202010133
[4] M. Koch, D.M. Mittleman, J. Ornik, E. Castro-Camus, Nat. Rev. Meth. Primers, **3**, 48 (2023). DOI: 10.1038/s43586-023-00232-z
[5] H. Huang, Z. Liu, M.T. Ruggiero, Z. Zheng, K. Qiu, S. Li, Zu. Zhang, Zi. Zhang, Cryst. Growth Des., **25**, 3578 (2025). DOI: 10.1021/acs.cgd.4c01423
[6] *Terahertz optoelectronics*, ed. by K. Sakai (Springer, Berlin–Heidelberg, 2005). DOI: 10.1007/b80319
[7] A.V. Andrianov, Phys. Solid State, **65** (10), 1563 (2023). DOI: 10.61011/PSS.2023.10.57208.142.
[8] A.V. Andrianov, A.N. Aleshin, S.N. Abolmasov, E.I. Terukov, E.V. Beregulin, JETP Lett., **116** (12), 859 (2022). DOI: 10.1134/S0021364022602585.
[9] A.V. Andrianov, A.N. Aleshin, S.N. Abolmasov, E.I. Terukov, A.O. Zakhar'in, Phys. Solid State, **65** (5), 814 (2023). DOI: 10.21883/PSS.2023.05.56054.27.
[10] H.-T. Chen, R. Kersting, G.C. Cho, Appl. Phys. Lett., **83**, 3009 (2003). DOI: 10.1063/1.1616668
[11] A.V. Andrianov, A.N. Aleshin, V.N. Truhin, A.V. Bobylev, J. Phys. D, **44**, 265101 (2011). DOI: 10.1088/0022-3727/44/26/265101
[12] C. Song, P. Wang, Y. Qian, G. Zhou, R. Nötzel, Opt. Express, **28**, 25750 (2020). DOI: 10.1364/OE.400590
[13] A.A. Volfson, V.K. Subashiev, FTP, **1**, 397 (1967). (in Russian)
[14] A.S. Abramov, D.A. Andronikov, S.N. Abolmasov, E.I. Terukov, in *High-efficient low-cost photovoltaics*, ed. by V. Petrova-Koch, R. Hezel, A. Goetzberger (Springer, Cham, 2020), ch. 7, p. 113–132. DOI: 10.1007/978-3-030-22864-4_7
[15] G.E. Jellison, Jr., F.A. Modine, Appl. Phys. Lett., **41**, 180 (1982). DOI: 10.1063/1.93454

Translated by EgoTranslating